Encapsulation of Small Base Molecules and Tetrahedral/Cubane-Like Clusters of Group V Atoms in the Boron Buckyball: A Density Functional Theory Study

ARTICLE *in* THE JOURNAL OF PHYSICAL CHEMISTRY A · FEBRUARY 2011

Impact Factor: 2.69 · DOI: 10.1021/jp107630q · Source: PubMed

4 AUTHORS, INCLUDING:

Jules Tshishimbi Muya
University of Richmond
19 PUBLICATIONS **164** CITATIONS
SEE PROFILE

Minh Tho Nguyen
University of Leuven
748 PUBLICATIONS **10,861** CITATIONS
SEE PROFILE

Arnout Ceulemans
University of Leuven
252 PUBLICATIONS **4,106** CITATIONS
SEE PROFILE

THE JOURNAL OF PHYSICAL CHEMISTRY A

ARTICLE

pubs.acs.org/JPCA

Encapsulation of Small Base Molecules and Tetrahedral/Cubane-Like Clusters of Group V Atoms in the Boron Buckyball: A Density Functional Theory Study

Jules Tshishimbi Muya,* Erwin Lijnen, Minh Tho Nguyen, and Arnout Ceulemans

Department of Chemistry and Institute for Nanoscale Physics and Chemistry (INPAC), University of Leuven, Celestijnenlaan 200F, B-3001 Leuven, Belgium

Supporting Information

ABSTRACT: A density functional theory study of small base molecules and tetrahedral and cubane-like group V clusters encapsulated in B_{80} shows that the boron buckyball is a hard acid and prefers hard bases like NH_3 or N_2H_4 to form stable off-centered complexes. In contrast, tetrahedral and cubane-like clusters of this family are metastable in the cage. The most favorable clusters are the mixed tetrahedral and cubane clusters formed by nitrogen and phosphorus atoms such as $P_2N_2@B_{80}$, $P_3N@B_{80}$, and $P_4N_4@B_{80}$. The boron cap atoms are electrophilic centers, and prefer mainly to react with electron rich nucleophilic sites. The stability of the complexes will be governed by the size and electron donating character of the encapsulated clusters. B_{80} forms stable complexes with hard materials where a bidentate interaction of the encapsulated molecule with two boron cap atoms is preferred over a single direct complex toward a single endohedral boron.

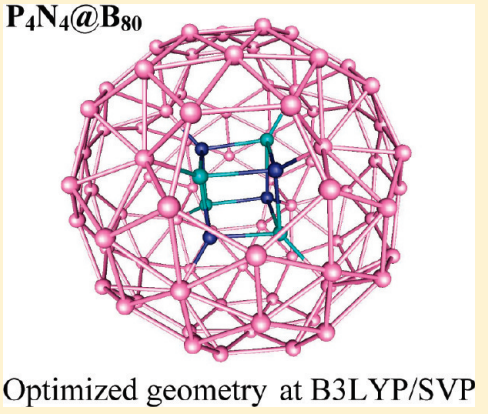

INTRODUCTION

A new highlight in the research on buckyballs and fullerenes is the recent claim that the boron buckyball B_{80}, consisting of 80 boron atoms with a shape similar to the celebrated C_{60}, could be a new stable allotrope of boron.[1] The geometry,[2−4] physical and chemical properties of B_{80}[5−10] are being studied extensively and potential applications are already anticipated. According to calculations B_{80} should present promising prospects for electronic transmission, hydrogen storage, and electronic conductivity when solid state B_{80} is doped with Mg or alkali metals.[11−16] The equilibrium geometry of B_{80} computed at the B3LYP/6-31G(d) level is slightly distorted from icosahedral symmetry to T_h symmetry.[2] In a valence bond picture, B_{80} is isoelectronic to C_{60}. The electron deficient truncated icosahedral B_{60} frame is saturated through an extra B_{20} orbit, which has the shape of a dodecahedron and caps all hexagons.[5] Li et al.[17] investigated alternative B_{80} structures, starting from a stable icosahedral B_{12} core surrounded by 68 outer boron atoms. The outer shell was subsequently minimized using a basin-hopping Monte Carlo procedure. They found a core−shell B_{80} cluster which is ∼1.6 eV more stable than the boron buckyball at the TPSS/6-311G-(2d)//PBE/GTH-DZVP level. Along similar lines, a recent molecular dynamics simulated-annealing analysis, with further optimization within PBE/DND, yielded an analogous core−shell B_{80} cluster, also containing an inner B_{12} icosahedron surrounded by an incomplete B_{68} outer shell. This structure is energetically ∼2.3 eV below the buckyball B_{80}.[18] The B_{12} core with outer B_6/B_7 pyramidal structures has however characteristics, which relate it to solid ss-boron. Clearly, these solutions represent an intermediate step in the growth process of solid boron, and lack the unique "magic" electron count of the buckyball allotrope. The higher stability is related to the slightly higher coordination number of the electron deficient boron atoms in the core−shell structure as compared to the hollow clusters. Because of the incomplete nature of the outer shell, it is likely that both reported core−shell structures belong to one large minimal energy basin on the potential energy surface, with many nearby conformations. In contrast, the buckyball structure represents a deep local minimum with a unique character. Hence this finding does not exclude the viability of the boron fullerene B_{80}. Note that C_{60} is also an energetically higher-lying allotrope of carbon when compared to diamond and graphite.

Recently, we demonstrated the viability of substituted boron buckyballs, where some capping borons are replaced by methyne fragments, which also can share three valence electrons with the bonding network. The most stable substitution patterns correspond to structures in which 4 or 8 caps forming a tetrahedron or a cube are replaced by methyne fragments. Interestingly in the resulting $B_{80-x}(CH)_x$ ($x = 4, 8$) clusters 12 boron caps are pointing outward (exohedral), while the remaining caps are pointing inward (endohedral). This radial distortion pattern is similar to the $I_h \rightarrow T_h$ stabilization mode calculated for B_{80}. The driving force for both the distortion mode and the substitution pattern seems to be the formation on the surface of six B_4 motifs which are characterized by

Received: August 12, 2010
Revised: November 26, 2010
Published: February 25, 2011

a strong 4-center bond. The endohedral orientation of the remaining caps provides anchor points for encapsulated tetrahedral and cubane-like clusters.[9] Encapsulation of atoms and molecular fragments in C_{60} is well documented, both theoretically and experimentally. Endohedral compounds have many potential applications in nanoelectronics, drug delivery, radioactive tracers, and energy storage. Since buckminsterfullerene C_{60} is chemically electronegative, it forms endohedral complexes with atoms or molecules that donate electrons to the frame. Alkali metals and transition metals, encapsulated in fullerenes, yield a rich collection of fascinating compounds.[19−27] As an example chemists recently isolated a "Russian doll" metallofullerene $C_2@Sc_4@C_{80}$.[28] Along similar lines, theoretical studies predict the stability of endohedral boron nanostructures $Fe@B_{80}$ and $Ni@B_{80}$.[29,30] These molecules are potential single molecule devices possessing tunable electronic structures and magnetic properties depending on the metal and its position in the B_{80} cavity. $ScN_3@B_{80}$ and $La@B_{80}$ have also been predicted to be stable with interesting physical properties.[31] As compared to carbon fullerenes, boron fullerenes have a larger diameter and contain reactive endohedral caps. This should make them more suitable for encapsulation of small organic and inorganic molecules and molecular fragments. Research in this direction has been performed by Jemmis et al.,[3,32] who investigated the boron buckyball stuffed with *closo*-boron clusters. The present paper investigates the electronic structure and stability of embedded tetrahedral and cubane-like clusters particularly of group V elements. In our study we will focus on the encapsulation of the tetrahedral clusters N_4, P_4, As_4, Sb_4, and derivatives such as P_2N_2, P_3N, and the cubane-like clusters P_8, P_4C_4, P_4N_4, and B_4N_4. We also examine the complexation of ammonia, phosphine, arsine, hydrazine, and ammonia borane on the endohedral boron sites. Furthermore, we compare endohedral boron fullerenes with endohedral carbon fullerenes encapsulating the same molecules. The aim is to understand the very special chemical properties of the boron buckyball cavity, which may stabilize unusual conformations of the encapsulated molecules, and give rise to the fabrication of novel materials.

METHOD

DFT calculations of type B3LYP/STO-3G, B3LYP/SVP,[33] B3LYP/def2-TZVPP,[34,35] and B3LYP/6-31G(d) were used for geometry optimization to obtain results at different levels of theory and to minimize the computational cost. Harmonic vibration frequencies were first computed at the small basis set B3LYP/STO-3G and then at larger basis sets B3LYP/SVP or B3LYP/6-31G(d) in order to characterize the nature of the stationary points and to determine the zero-point vibration energy corrections by analytical evaluation of the second derivative of the energy with respect to nuclear displacements. The hybrid density functional method B3LYP was chosen to include electron correlation in the accurate prediction of the geometry. All calculations were carried out with the Gaussian 03[36] and TURBOMOLE-V-5−10[37] packages. The gOpenmol[38,39] and g molden programs[40] were used to visualize the total electron density, the molecular orbitals and the equilibrium geometries. The distribution of charges on different atoms in the endohedral boron fullerenes were calculated at B3LYP/6-31G(d) level by the NBO program.[41] Starting geometries were usually based on symmetry considerations with heteroatoms either pointing toward the endoboron caps, or toward the exocaps. Symmetry constraints were relaxed during the optimization. The frequency analysis of high symmetry extremal points were calculated at a large basis set level of theory, whereas the frequencies of the optimized lower symmetry endohedral boron fullerenes were calculated using a lower basis sets. We have plotted the molecular graph with the AIM2000 program[42] to identify both the bond critical points and the ring critical points in the $P_4@B_{80}$ complex.

RESULTS

A. Endohedral Ammonia and Phosphine. The encapsulated $N@C_{60}$ and $P@C_{60}$ complexes were discovered in 1995 by Weidinger et al.[43−46] It was shown by quantum chemical calculations that the wave functions of the N and P atoms do not mix with the wave function of the fullerene molecule, implying that these atoms do not bind to the cage. Turning to the boron homologues, we expect stronger interactions between the group V heteroatoms and the cage, since it is well-known that amines and phosphines can form donor−acceptor bonds with boron. Nguyen et al.[47] have recently intensively studied aminoborane complexes for hydrogen storage applications. The BH_3 is electron-deficient and is expected to form stable complexes with electron-rich systems with base character. As an example, in Table 1, we list the typical characteristics of the B−N, B−P, B−As, and B−Sb bonds, HOMO−LUMO gap energies, complexation energies and charges transferred in small complexes as H_3N-BH_3, $H_4N_2-BH_3$, H_3P-BH_3, $P_4-(BH_3)_4$, $(CH_3)_3P-BH_3$, H_3As-BH_3, $As_4-(BH_3)_4$, H_3Sb-BH_3, and $Sb_4-(BH_3)_4$. Two important properties seem to control the stability of these complexes. The complexation energies in the hydride series H_3N-BH_3, H_3P-BH_3, H_3As-BH_3, H_3Sb-BH_3 decrease with increasing size of the heteroatom. This points to the importance of polarizability: larger atoms, which are more polarizable form less stable complexes. The same trend is observed for the series $P_4-(BH_3)_4$, $As_4-(BH_3)_4$, $Sb_4-(BH_3)_4$. On the other hand for a given heteroatom the basicity can be increased by introducing further substituents, and this again will give a larger complexation, as shown by the complexes with hydrazine and $P[(CH)_3]_3$. The experimental P−B bond length amounts to 1.937 Å,[48] which is in very good agreement with the calculated B−P bond distance of 1.935 Å at B3LYP/def2-TZVPP in H_3P-BH_3. Anane et al.[49] have also studied these and similar complexes and found that the complex $(CH_3)_3P-BH_3$ is more stable than H_3P-BH_3 and that the B−P bond lengths in these two complexes are 1.945 and 2.019 Å respectively for H_3P-BH_3 and $(CH_3)_3P-BH_3$ at the MP2(full)/6-31G(d) level. The exchange functional B3LYP combined with def2-TZVPP describes quite well the equilibrium geometries of these complexes compared to the post Hartree−Fock full MP2 at the 6-31G(d) level. It was argued that PH_3 is a harder base than $(CH_3)_3P$ and that the boron hydride BH_3 which is known as a soft acid prefers a soft base in line with the softness and hardness principle of Pearson.[50] The change in B−P bond distances observed in these structures may reflect the relative strengths of these interactions. Consequently, the P_4 which interacts weakly with the BH_3 can be considered as a harder base than $(CH_3)_3P$ and PH_3. Next we have inserted the same ligands in the boron buckyball. Optimized geometries of those complexes are described in Table 2.

Ammonia, phosphine, hydrazine, and ammonia borane molecules can form thermodynamically favorable complexes with B_{80}. H_3N-B_{80} is the most stable complex in this series with a large HOMO−LUMO gap and appreciable formation energy. In contrast, complexation of the ammonia borane is virtually

Table 1. Bond Lengths, Complexation Energies, and HOMO−LUMO Gaps Computed at the B3LYP/SVP Level, and Charge Distribution at the 6-31G(d) Level for Some Borane Complexes of Hydrides of group V Elements[a]

complexes	heteroatom−B bond lengths (Å)	complexation energies (kcal/mol)	charges on heteroatom	charges on B	HOMO−LUMO gap (eV)
H_3N-BH_3	1.65	−35.82	−0.95	−0.17	7.51
H_3P-BH_3	1.95 (1.937)[48]	−23.53	0.55	−0.65	8.70
H_3As-BH_3	2.10	−15.89	0.55	−0.55	8.50
H_3Sb-BH_3	2.33		0.94	−0.54	7.80
$H_4N_2-BH_3$	1.70	−42.04	−0.71; −0.65	−0.24	7.86
$(CH_3)_3P-BH_3$	1.93	−36.95	1.42	−0.70	8.01
$P_4-(BH_3)_4$	2.08	−17.57	0.36	−0.41	5.58
$As_4-(BH_3)_4$	2.45	−8.35	0.40	−0.45	4.68
$Sb_4-(BH_3)_4$	2.76	2.75	0.26	−0.15	3.81

[a] The Sb−boron complexes have been computed at the B3LYP/def-SVP level. The charge of the Sb complex was calculated at the B3LYP/STO3-G level.

Table 2. Bond Lengths, HOMO−LUMO Gaps, Charge, and Complexation Energies of $H_3N@B_{80}$, $H_3P@B_{80}$, $H_3As@B_{80}$, $H_4N_2@B_{80}$, $H_3NBH_3@B_{80}$, and $(CH_3)_3P@B_{80}$ Complexes at the B3LYP/SVP Level

complexes	heteroatom-B bond lengths (Å)	complexation energies (kcal/mol)	charges on heteroatom	charges on B	HOMO−LUMO gap (eV)
$H_3N@B_{80}$	1.61	−27.09	−0.98	0.36	1.82
$H_3P@B_{80}$	1.98, 2.05	−11.30	0.60	−0.13; −0.06	0.70
$H_3As@B_{80}$	3.25	5.83	0.20	0.19	1.97
$H_4N_2@B_{80}$	1.62	−24.35	−0.68, −0.64	0.37	1.75
$H_3NBH_3@B_{80}$	1.56	−0.15	−0.94	0.17; 0.22[a]	1.88
$(CH_3)_3P@B_{80}$	1.94	118.27	1.54	−0.19	1.81

[a] Charge of cap boron attached to ammonia borane by a hydrogen bond.

thermo-neutral. The ammonia molecule is a hard base. Hardness decreases in the PH_3, AsH_3 and SbH_3 series for reason for higher polarizability. Clearly, as compared to Table 1, the results in Table 2 relate to two separate energetic effects. On the one hand bond formation takes place between the group V heteroatom and the endoboron caps, which will be governed by acid−base properties. On the other hand the data also reflect the steric strain from the cavity. As far as base properties are concerned, BH_3 and B_{80} are quite different. BH_3 is commonly regarded as a soft acid. In contrast, in B_{80} the cap atoms loose electrons to the framework, thus increasing their acidity.[5] As a consequence, ammonia, which is the hardest base, is expected to form the strongest bond. In $NH_3@B_{80}$, $H_3P@B_{80}$, $H_4N_2@B_{80}$, and $(CH_3)_3P@B_{80}$ complexes, ligands leave the central position and move to the acid cap boron atom to form a strong B−N or P−N bond with the cage, unlike the AsH_3 which prefers to stay in the middle of the cage. All these encapsulated molecules keep the compact structures except for the PH_3 molecule in the phosphine@B_{80} complex. The complex $H_3P@B_{80}$ has a favorable complexation energy of −11.30 kcal/mol. Nevertheless the encapsulation profoundly changes the shape of the PH_3 base. It dissociates into PH_2 and H fragments which are attached to different endohedral capping atoms of the cage. The total charges on the PH_2 and H fragments are, respectively, +0.69 and −0.03. The B_{80} cage captures around 0.66 electrons from the PH_3 (PH_2+H) ligand. Similar dissociation was observed at B3LYP/SVP with the organic molecule CH_3SH encaged in B_{80}. The CH_3SH dissociates in CH_3S and H fragments, with positive +0.40 and negative −0.03 charges, respectively; both fragments are attached to different cap boron atoms on the B_{80} cage. Such dissociation is prevented in the methylated phosphorus compound, but the formation of $(CH_3)_3P@B_{80}$ is thermodynamically unfavorable due to the fact that the methyl groups are too big and the steric effects increase the strain in the cage. For comparison, we have studied the endohedral ammine and hydrazine complexes, as examples of a nitrogen base. This yields strong donor−acceptor bonding with respectively −27.09 and −24.35 kcal/mol. Nonetheless this value is higher than the bond energy of −42.04 and −35.82 kcal/mol for the B−N bond in the $H_4N_2BH_3$ and BH_3NH_3 molecule computed at the same B3LYP/SVP level of theory (Table 1). Also the B−N bond length of 1.65 Å in ammonia borane is close to the B−N bond distance in hydrazine@B_{80} and ammonia@B_{80}. The encapsulated hydrazine molecule transfers nearly 0.37 electrons to B_{80} and the N−N bond length is similar to the N−N hydrazine and hydrazine-BH_3 bond lengths of 1.47 Å calculated at the same level of theory. The experimental value for hydrazine is 1.45 Å.[51]

B. Endohedral N_4, P_4, P_3N, and P_2N_2 Clusters Encaged in B_{80}. Tetrahedral N_4 is an elusive molecule with an energy 186 kcal/mol above that of two separate N_2 molecules and with a 61 kcal/mol barrier between the two species.[52] Yarkony indicated that the barrier energy between $2N_2$ and N_4 can be reduced to approximately 28 kcal/mol due to spin−orbit coupling with the triplet state.[53] This molecule could be a potential high-energy-density fuel for nonpolluting supersonic transport. Interestingly encapsulation in a boron or carbon cage could provide a strategy to isolate tetrahedral N_4. Endohedral fullerene complexes such as $N_4@C_{60}$ and $N_4@C_{80}$ were thoroughly studied. In these compounds the N_4 cluster is situated in the center of the cage. It was found that N_4 did not interact with the carbon cage and that the HOMO and LUMO are both localized on the C_{60} or C_{80} cage.[54,55] On the other hand, for C_{80}, Chun-Mei et al. showed that the N_4 cluster encaged in C_{80} stabilizes the system

and quenches the magnetism of the system to become nonmagnetic.[55]

Figure 1 shows the equilibrium geometries of encapsulated N_4 in the boron cage. Two geometries lie at the bottom of the potential energy surface with total electronic energies of −2203.1418 hartree and −2203.1545 hartree, depending on the orientation of the N_4 cluster in the cage. The higher energy corresponds to the geometry of (Figure 1a), where one N atom is linked to an endo boron cap atom and the N_4 cluster occupies an off-center position. Clearly the formation of the N−B bond is a special feature of the boron buckyball, which has no counterpart in the carbon fullerenes. However the cap boron attached to the N_4 has a charge of +0.25, which is 0.10 higher than the remaining caps and the charge of the N atom involved in the B−N bond becomes slightly negative with −0.036 charges. The nitrogen atom is more electronegative than the boron atom and tends to take electrons from the B_{80} cage. The $N_4@B_{80}$ complex with N_4 in the center (Figure 1b) is nearly 7.95 kcal/mol lower in energy. The N atoms are oriented toward the exo boron cap atoms and the complex resembles the previous $N_4@C_{60/80}$ complexes. A comparison of bond lengths, angles and positions in $N_4@B_{80}$ complexes and similar carbon compounds is given in Table 3. The bond distances and angles of the embedded N_4 cluster are all in the same range with N−N bond distances of 1.46 Å at CCSD(T)/TZ2Pf and 1.45 Å at B3LYP/TZ2Pf in the isolated N_4 compound reported in ref 56, approaching the N−N bond distance of 1.48 Å in metastable tetrahedral N_4H_4.[57,58] The geometry of the B_{80} cage encapsulating the N_4 molecule is still similar to pristine B_{80}; only the cap boron atom attached to N is subject to an inward displacement of 0.60 Å and forms a strong B−N bond, which increases the stability of the complex. The tetrahedral N_4 in B_{80} retains a compact shape. A similar shape has been observed in $N_4@C_{60}$ and $N_4@C_{80}$. Compact shapes are also found in comparable compounds such as $ZrH_4@C_{60}$[59] and $CH_4@C_{60}$.[60] In the off-center compound, the formation of a B−N bond with the capping boron also leads to an elongation of the B−B bonds in the capping hexagon. The distribution of charges computed by the NBO program indicates that the four N atoms in N_4 placed off-center transfer nearly 0.19 electrons to the boron buckyball cage. The centered N_4 cluster did not transfer any electrons to the boron cage. The B−N bond of 1.60 Å observed in the a-$N_4@B_{80}$ isomer complex approaches the B−N bond length of 1.61 and 1.62 Å of H_3N-B_{80} and hydrazine-B_{80} complexes shown in Table 2. The N_4 seated in the center of the B_{80} does not interact with the cage. The same result was observed in $N@C_{60}$, $N_4@C_{60}$ and $N_4@C_{80}$.[54,55,61,62] Apparently, in the case of the b-$N_4@B_{80}$, isomer interactions with the cage are weak because of the small size of the tetrahedron N_4 compared to the diameter of the cage. This is reflected by the small amount of charge transferred between the centered N_4 cluster and the cage. The B_{80} cage in the centered complex is less distorted. This fact has a favorable impact on lowering the energy of the complex.

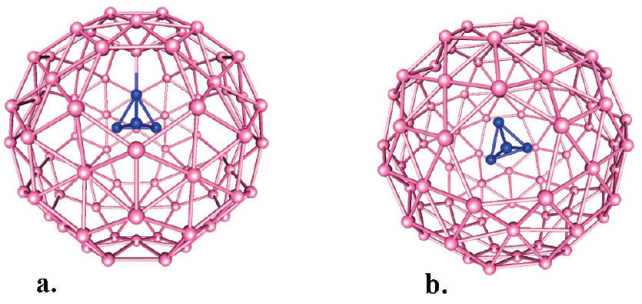

Figure 1. Optimized geometries of $N_4@B_{80}$ at the B3LYP/SVP level: (a) off centered complex; (b) centered complex.

Elementary phosphorus exists in two forms: the red metastable and the white stable phosphorus. The latter consists of tetrahedral P_4 molecules. It is a key industrial intermediate for most phosphorus compounds of commercial importance. White phosphorus is extremely reactive to oxygen, but recently it was demonstrated that it could be prevented from oxidation by encapsulation in a tetrahedral cage complex.[63] As compared to N_4 the size of P_4 is increased significantly, and the softness also increases.

Figure 2 depicts the equilibrium geometries of $P_4@B_{80}$ complexes optimized by DFT calculations at the B3LYP/SVP level of theory. Three extreme geometries—all three local minima—are found that differ by the shape of the P_4 cluster embedded in the cage. In the tetrahedral $P_4@B_{80}$ shown in (Figure 2a), the P_4 cluster keeps the tetrahedral symmetry and each phosphorus atom is bound to one endohedral cap boron of the B_{80} cage. The second P_4 isomer in (Figure 2b) is strongly distorted with two broken P−P bonds and each phosphorus atom is linked to two boron atoms of the boron cage. This geometry resembles a bisphenoid or butterfly form. Another minimum lies between the two geometries and is shown in (Figure 2c). This geometry is characterized by a three-membered phosphorus ring with the fourth phosphorus attached to one vertex. Of the four phosphorus atoms in the c-isomer, two phosphorus atoms are linked to two cap boron atoms like for the bisphenoid, and the two others are bound to only one boron like in the tetrahedral complex $P_4@B_{80}$. The c-isomer is the lowest in energy with a

Table 3. Geometry of $N_4@B_{80}$, B_{80} and N_4 at the B3LYP/SVP Level and Analogous Fullerene Complexes[a]

geometry parameters	$N_4@B_{80\ (a)}C_1$	$N_4@B_{80\ (b)}C_1$	$N_4@C_{60}$[54]	$N_4@C_{80}$[55]	B_{80}[2]	N_4 T_d
N−N bond lengths (Å)	1.44−1.46	1.43−1.44	1.44	1.48		1.44; 1.45;[54] 1.48[57]
N−N−N bond angles (°)	59.5−60.9	59.9−60.1	60	60		60[52,57]
N−B bond lengths (Å)	1.60					
B−B 6−5 bond lengths (Å)	1.67−1.77	1.72−1.77			1.76	
B−B 6−6 bond lengths (Å)	1.65−1.68	1.65−1.68			1.68	
nearest B−N distance (Å)	1.60	2.97				
center to nearest endo-B	3.07 (0.60)	3.68			3.67	
center to exo-B	4.04 (0.10)	3.97			3.94	
central position	no	yes	yes	yes		

[a] In parentheses are the deviations of nearest and furthest boron atoms to the reference B_{80} caps.

dx.doi.org/10.1021/jp107630q |J. Phys. Chem. A 2011, 115, 2268–2280

total electronic energy of −3349.4780 hartree, followed by the b-isomer and a-isomer respectively with −3349.4606 hartree and −3349.4415 hartree. Compared to the triangular structure (Figure 2c), the bisphenoid structure (Figure 2b) is 10.92 kcal/mol higher in energy, and the tetrahedral structure (Figure 2a) is 22.98 kcal higher in energy. Table 4 shows the geometrical parameters of the three optimized isomers of the complex $P_4@B_{80}$. Figure 3 offers a more detailed view of the bonding to the cage. The P−P−P bond angle in a tetrahedral P_4 molecule is around 60°. This very sharp angle produces a considerable amount of strain. The tetrahedral $P_4@B_{80}$ *a*-isomer has a geometry only slightly distorted compared to the isolated molecules P_4 and B_{80}. However in the b-isomer and c-isomer the strain is relieved to form a bisphenoid or triangular structure by the rupture of two opposite or two adjacent P−P bonds, respectively. The loss of bonding is compensated by the formation of bidentate addition to two neighboring endo caps. By analyzing carefully the energies of the B_{80} cage and the embedded P_4 we have found that the tetrahedral geometry of P_4 seated in B_{80} is very close to the optimized P_4 geometry with a marginal difference in total electronic energy of 0.57 kcal/mol at the same level of theory. On the other hand the encapsulation strongly distorts the B_{80} cage. The deformation energy of B_{80} by the complexation reaction in this a-isomer is nearly 38.12 kcal/mol. For the bisphenoid structure the bond rupture gives rise to a much higher deformation energy of about 207.65 kcal/mol compared to neutral P_4, but this is of course compensated by bond formation and electron transfer. Still the gain in energy carried by the formation of 8 B−P bonds in the complex is not sufficient to yield overall negative complexation energy. Hence, the formation of all $P_4@B_{80}$ complexes is still endothermic, with formation energies of 57.57 kcal/mol, 45.52 and 34.59 kcal/mol respectively for the tetrahedral, bisphenoidal and triangular symmetries. The vibration frequencies of the tetrahedral isomer have been calculated at B3LYP/SVP to check if we have reached the minimum at the potential energy surface. The lowest real frequency vibration mode of the tetrahedral complex amounts to 16 cm^{-1} and corresponds to the twisting mode of P_4 inside the cage, the bisphenoid structure and the triangular c-isomer show

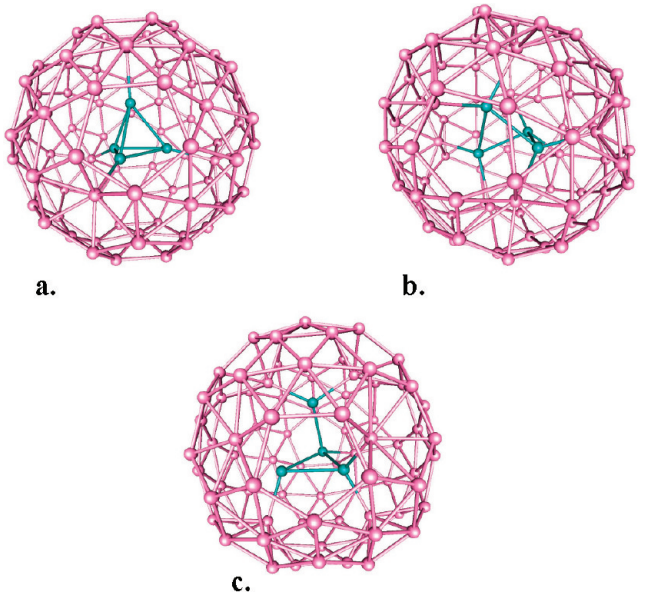

Figure 2. Optimized $P_4@B_{80}$ complexes at the B3LYP/SVP level: (a) central position with *T* symmetry; (b) bisphenoid type; (c) triangular type.

Table 4. B3LYP/SVP Optimized Parameters of $P_4@B_{80}$, B_{80}, and T_d P_4[a]

geometry parameters	$P_4@B_{80}$ (a) T	$P_4@B_{80}$ (b) C_1	$P_4@B_{80}$ (c) C_1	B_{80}[2]	P_4
P−P bond lengths (Å)	2.21	1.93−2.17	2.12−2.26		2.22; 2.18[64]
P−B	1.98	1.93−2.17	1.84−1.97		
P−P−P bond angles (deg)	59.06−60.47	74.44−74.84	58.47−78.38		60[64]
B−B 6−5 bond lengths (Å)	1.70−1.75	1.66−1.80	1.60−1.87	1.76	
B−B 6−6 bond lengths (Å)	1.65−1.69	1.64−1.69	1.61−1.74	1.68	
shortest B−P bond distance (Å)	2.01	1.93	1.85		
center-nearest B	3.30 (0.37)	3.19 (0.48)	2.92 (0.75)	3.67	
center-furthest B	4.05 (0.11)	4.20 (0.26)	4.30 (0.36)	3.94	
off center position of the cage	no	no	no		

[a] In parentheses are the deviations of nearest and furthest boron atoms to the reference B_{80} caps.

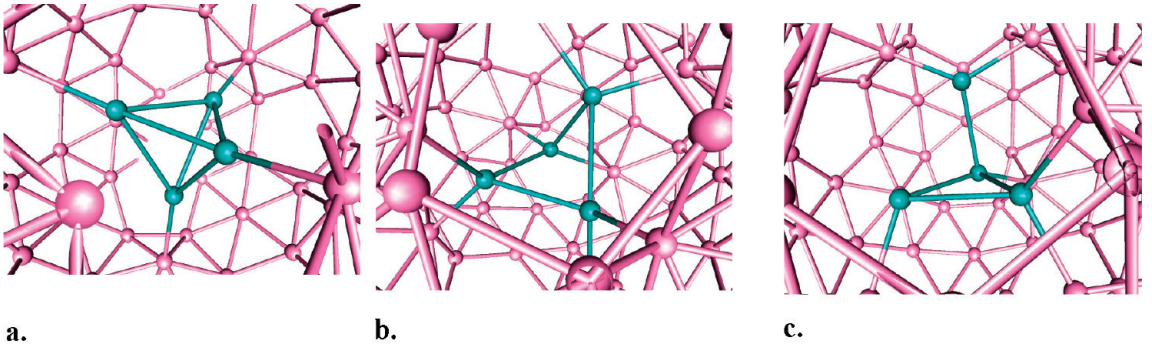

Figure 3. Detailed view of encaged P_4 clusters in the B_{80} cage: (a) central position with *T* symmetry; (b) bisphenoid type; (c) triangular type.

also a low-frequency twisting mode localized respectively at 145 and 119 cm^{-1} at the B3LYP/STO-3G level. All frequencies in these three complexes are real respectively at B3LYP/SVP and B3LYP/STO-3G levels. The distributions of charges calculated at B3LYP/6-31G(d) by NBO in the three isomers indicate that the P_4 atoms transfer nearly 2 electrons to the boron cage. The molecular graph of the tetrahedral complex $P_4@B_{80}$ is depicted in (Figure 4). The Bader atoms in molecules theory AIM argues that the properties of molecular charge distribution are summarized in terms of its critical points.[65−68] The analysis of the bond critical points carried out by the AIM2000 program at the STO-3G level on tetrahedral $P_4@B_{80}$ suggests that the bond critical point (BCP) of each B−P bond lies nearer to the cap boron atom. The B−P bonding is a mixture of an ionic and covalent bond since the electron density at BCP along the B−P bond shown in Figure 4 lies in the range of intermediate interaction defined in refs 64 and 69, characterized by an electron density $0.07 < \rho < 0.15$, an absolute ratio of principal curvatures $\lambda_1/\lambda_3 < 0.20$ with $\lambda_1 < \lambda_2 < \lambda_3$, a positive Laplacian of electron density and a negative total electronic energy. The positive value of the Laplacian expresses that electrons are depleting at that BCP.

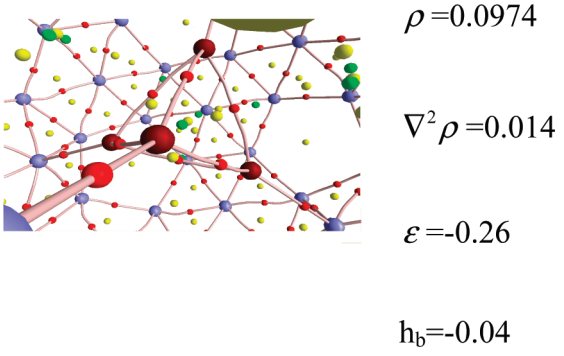

Figure 4. Section of molecular graph of tetrahedral $P_4@B_{80}$ complex. The boron atoms and phosphorus atoms are respectively in green and maroon color. The critical points between the phosphorus atom and the boron atoms along the bond B−P are in red.

In Table 5, the optimized geometries of $P_2N_2@B_{80}$ and $P_3N@B_{80}$ complexes are presented. The phosphorus atoms in these structures are bound to two boron atoms, as is the case in the bisphenoid complex $P_4@B_{80}$ (Figure 5). We have found two $P_3N@B_{80}$ isomers: a four-membered ring N_3P and a three-membered ring N_3P (Figure5, parts a and b) with nearly thermo-neutral complexation energies of 1.14 and 3.77 kcal/mol respectively for the b-isomer and a-isomer at B3LYP/SVP. In P_2N_2 the unique P−P bond breaks and allows the formation of an open chain P_2N_2 that stabilizes thermodynamically the complex with a complexation energy of −24.91 kcal/mol (Figure 5c). The N−N bond length encountered in the $P_2N_2@B_{80}$ complex is only 0.07 Å shorter than that of hydrazine@B_{80} and cyclotetrazanes.[57] The three complexes shown in Figure 5 have the following electronic energies: −2776.3879 hartree for $P_2N_2@B_{80}$, −3062.9367 hartree for the a-isomer $P_3N@B_{80}$ and −3062.9409 for the b-isomer $P_3N@B_{80}$.

Table 5. B3LYP/SVP Optimized Parameters of $P_2N_2@B_{80}$, $P_3N@B_{80}$, B_{80} and P_2N_2[a]

bond and angles	$P_3N@B_{80}$ (a)	$P_3N@B_{80}$ (b)	$P_2N_2@B_{80}$	B_{80}	P_2N_2[70] theor
P−N bond lengths (Å)	1.83, 1.81	1.85−2.04	1.88, 1.91		1.68
P−B (Å)	1.98−2.11	1.93−2.09	2.02, 2.16		
N−N (Å)			1.41		2.46
P−P (Å)	2.34	2.15			2.20
N−B (Å)	1.44	1.60−1.88	1.66, 1.39		
N−P−N bond angles (deg)			82.70		
N−N−P (deg)			91.01, 90.27		
B−B 6−5 bond lengths (Å)	1.64−1.80	1.64−1.81		1.76	
B−B 6−6 bond lengths (Å)	1.64−1.72	1.64−1.71		1.68	
shortest B−P bond distance (Å)	1.99	1.93			
center-nearest B (Å)	2.73 (0.94)	2.70 (0.97)	2.88 (0.79)	3.67	
center-furthest B (Å)	4.15 (0.21)	4.31 (0.37)	4.18 (0.24)	3.94	
off-center position	no	no	no		

[a] In parentheses are the deviations of nearest and furthest boron atoms to the reference B_{80} caps.

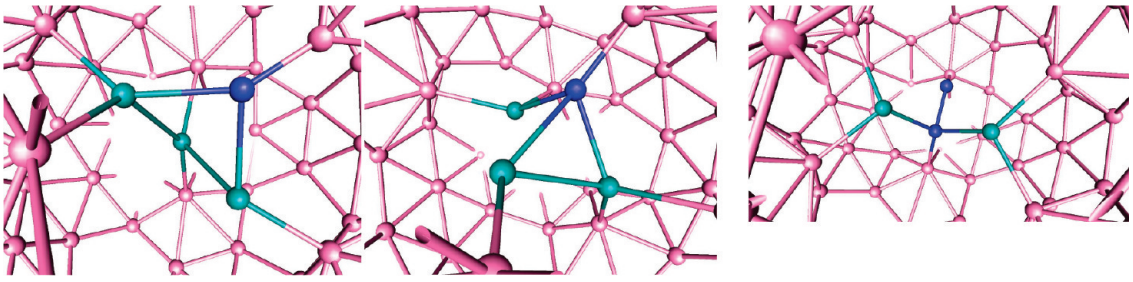

Figure 5. Detailed view of $P_3N@B_{80}$ (a, b) and $P_2N_2@B_{80}$ (c) complexes.

dx.doi.org/10.1021/jp107630q |J. Phys. Chem. A 2011, 115, 2268–2280

On the basis of the complexation energy the mixed phosphorus−nitrogen complexes appear more stable compared to their homologous tetrahedral phosphorus−boron and nitrogen−boron complexes. The lowest frequencies are localized at 163 cm^{-1}, 97 and 121 cm^{-1} respectively for a-isomer $P_3N@B_{80}$, b-isomer $P_3N@B_{80}$, and $P_2N_2@B_{80}$ at lower level. This confirms their vibrational stability.

In the a-isomer compared to the b-isomer, the B−N and P−N bonds are slightly shorter, whereas the P−B bonds and the P−P bonds are slightly longer. In all these complexes, the P−N bonds are more elongated than the calculated and experimental P−N bond in P_2N_2 and its derivatives reported in refs 70 and 71. However, for the encapsulated compounds, two phosphorus atoms are linked to two boron atoms to increase the stability. In the a-isomer of $P_3N@B_{80}$ the nitrogen atom is linked to two phosphorus atoms, and two P−P bonds are present, while in the b-isomer the nitrogen is linked to three phosphorus atoms and only one P−P bond remains. The substitution of one or two phosphorus atoms in $P_4@B_{80}$ by nitrogen has a favorable effect on the stabilization of the B_{80} complexes. In many cases studied in the present work, the most favorable complexation mode for an endohedral nucleophile seems to be edge-on to the center of a 6−6 bond, in between two neighboring boron caps.

C. Endohedral $As_4@B_{80}$ and $Sb_4@B_{80}$. The preceding results show that the optimal size for encapsulation probably lies between nitrogen and phosphorus. To study the strain effect of larger sizes, we have also computed the larger members of the series, As_4 and Sb_4. Arsenic vapor As_4 is an important material in semiconductor technology. Its chemical and physical properties have been thoroughly studied.[72−77] Sb_4 has only been observed in gas phase and *in silico*.[78,79] Four $As_4@B_{80}$ optimized structures have been found: the tetrahedral complex with T symmetry (a-isomer), the bisphenoid complex with C_2 symmetry (b-isomer) and the pyramidal complexes with C_1 symmetry (c- and d-isomers) (Figures S1 and S2, Supporting Information). Only the latter two are local minima. The total electronic energies of these four complexes calculated at the same level of theory B3LYP/SVP showed that the total electronic energy of the bisphenoid complex is −10926.6339 hartree, some 13.21 kcal/mol lower in energy than the tetrahedral symmetry complex. The tetrahedral and bisphenoid complexes are quite similar to the homologous $P_4@B_{80}$ complexes; the small structural difference in bisphenoid As_4 comes from the difference in the sequence of bonds As−B formed by two bidentate and two monodentate cap atoms. The third complex has a pyramidal geometry and it is the lowest energy among these three isomers with a total electronic energy of −10926.6370 hartree; each As atom of this cluster forms two bonds with two neighboring boron cap atoms of B_{80}, except for one As atom which is not linked to any boron of the B_{80} cage. Like the third isomer the fourth isomer has a pyramidal geometry with the small difference that the previously nonlinked As atom is now linked to one boron cap atom. The distortion in this isomer is strong which raises the total energy by 4.77 kcal/mol. The As−As bonds in T-$As_4@B_{80}$ and C_1-$As_4@B_{80}$ complexes are shorter than the As−As bonds calculated in isolated As_4, indicating a compression of the cluster (Table S1, Supporting Information). The As−As bond of 2.46 Å calculated at B3LYP/SVP in As_4 is close to the experimental value of 2.44 Å[75] and the computed PBE/DND As−As bond of 2.50 Å reported in ref 76. The B−As bond distances calculated for the $As_4@B_{80}$ complexes are in the same range with the B−As bond length of 2.065, 2.04, and 2.03 Å reported by Chadha et al. in an X-ray structure analysis of three trimethylarsine−boron trihalide compounds: $(CH_3)_3As−BCl_3$, $(CH_3)_3As−BBr_3$, and $(CH_3)_3As−BI_3$.[77] The pyramidal complex is more distorted than the tetrahedral or bisphenoidal complexes. The orientation of As has an influence on the electron donating properties of the encaged cluster. If the As is oriented in the direction of a single boron cap, its ability of giving electrons to the boron cage is reduced as compared to a bidentate orientation where it acts as a base toward two boron caps. The same tendency is observed in all other tetrahedral encaged clusters of the group V family studied in the present work.

Three optimized $Sb_4@B_{80}$ structures have been produced by DFT calculations at B3LYP/def-SVP (Figure S3−S4, Supporting Information). Referring to Table S2 (Supporting Information) the calculated Sb−Sb distances of 2.868 Å in isolated Sb_4 at B3LYP/def-SVP match with the previously calculated Sb−Sb bond average 2.87 Å at the multireference single and double excitation configuration interaction (MRSDCI) level,[78] and 2.91 Å at the B3LYP/GGA level.[79] The Sb−Sb bonds for the T-$Sb_4@B_{80}$ symmetry complexes (a- and c-isomer) are longer in the B_{80} cage than in the isolated Sb_4. In contrast, the C_1-$Sb_4@B_{80}$ complex (b-isomer) is contracted. The boron atom attached to Sb in all three isomers is pushed outward due to the large dimension of the Sb_4 cluster. These structures differ from pristine B_{80} by the fact that in these complexes only four boron atoms are endohedral and 16 are oriented outward, in contrast with the B_{80} in which there are 8 endo and 12 exo cap boron atoms. Of the three $Sb_4@B_{80}$ isomers, the c-isomer is the highest in energy. The tetrahedral a- and c-isomers have respective total energies of −2005.7463 and −2005.7288 hartree. The difference in energy between the two geometries is quite small: 10.96 kcal/mol. The b-isomer has a total electronic energy of −2006.0541 hartree at the def-SVP level and lies 204.13 kcal lower than the c-isomer at the same level of theory. The c-isomer has multiple Sb−B bonds and the Sb−Sb bonds are quite long. The complexation energies of those complexes are very large due to the large size of the Sb_4 cluster. The interactions of Sb_4 cluster and the B_{80} cage in $Sb_4−B_{80}$ complexes are different. In c- and b-isomers, the guest Sb_4 is larger and tends to form multiple bonds with the cage to compensate the weakness of Sb−Sb bonds. Contrary to the general trend to form multiple endohedral bonds, the Sb atoms in the a-isomer prefer to bind to one cap boron atom, keeping a nice tetrahedral geometry. The deformation of the B_{80} cage is pronounced in the c-isomer. The b-isomer is a transition state with an imaginary frequency of *i132* cm^{-1} at the B3LYP/STO-3G level. The equilibrium geometry is strongly distorted and characterized by a lowest real frequency localized at 90 cm^{-1} at lower level. The enclosed Sb_4 cluster tends to occupy a large space consequently exerting a lot of strain on B_{80} cage, which finally opens. The complexation energy of the complex decreases slightly but is still positive.

D. Adamantane@endo$B_{76}C_4$. From the previous results, it is clear that bulky enclosures can exert a lot of strain on the cage, without however breaking it. This demonstrates the great resilience of the cage to distortions. As a further example of a tetrahedral enclosure we have introduced the adamantane unit. This molecule has a tetrahedral structure with four carbon atoms in favorable position for bonding to the cage. To meet these carbon bonds, we replace the B_{80} cage by the endo-$B_{76}(CH)_4$ substituted cage (Figure S5, Supporting Information). Previous study has shown that this is the most viable $B_{80-n}(CH)_n$ isomer.[9]

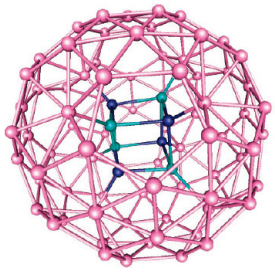

Figure 6. Optimized geometry of P_4N_4 @B_{80} at B3LYP/SVP.

The following isodesmic reaction was used to estimate the bonding energy of the complex:

$$endo\text{-}B_{76}(CH)_4 + TMA \rightarrow adam@endo\text{-}B_{76}C_4 + 4CH_4$$

where TMA represents the tetramethyladamantane.

The isodesmic energy is about 512 kcal/mol at the same level of theory B3LYP/SVP. This value is much higher compared to the highest value of formation energy observed among the tetrahedral complexes of family V elements. Clearly, the adamantane is too big to seat comfortably inside the endo-76 cage hollow. The C−C bond distances are contracted in this complex; the cage exerts pressure on the adamantane which destabilizes the complex, as is demonstrated by the positive isodesmic energy. Nonetheless this compound corresponds to a stable minimum. The adamantane core is contracted in the cage (Table S3, Supporting Information). The C−C and C−H bonds are shorter than the TMA (trimethyladamantane). The C−C and C−H bonds calculated in TMA at the B3LYP/SVP level are in the same range with the corresponding bonds in adamantane at the B3LYP/SVP and B3LYP/Aug-cc-pVDZ level.[80] The geometry of adam@endo-$B_{76}C_4$ is deformed; the carbon and boron frame of the endo-76 cage is pushed a little to the outside due to the large size of the adamantane molecule.

E. Endohedral Cubane-Like Clusters in the Boron Buckyball. In order to take advantage of the presence of eight endoboron caps, which could act as anchor points, we have also studied cubane-like compounds with eight group V atoms. In view of the importance of the size effect, which was revealed by the study of the tetrahedral compounds, we have limited our choice to the mixed P_4N_4 cluster and the homonuclear P_8. Furthermore, we also studied the insertion of the P_4C_4, and B_4N_4 clusters in the endo-$B_{76}C_4$ cage.

a. $P_4N_4@B_{80}$. The equilibrium geometry is shown in Figure 6. The P_4N_4 cluster sits in the center of the B_{80} cage. The phosphorus and nitrogen rich in electrons are bound to the cap boron atoms deficient in electrons. The equilibrium geometry is reached through different starting orientations of the P_4N_4 cluster inside the cage. The cubic conformation of the endohedral cluster is at variance with the normal conformation of the P_4N_4 cluster in other compounds, such as in cyclotetrahexaphosphazene, where it takes a cyclic nonplanar configuration with a six-membered ring.[81,82] Apparently the interaction with the boron caps favors this unusual conformation. The total electronic energy computed at the B3LYP/SVP level is nearly −3568.1715 hartree and yields a complexation energy of −32.87 kcal/mol with a HOMO−LUMO gap energy of 1.96 eV similar to B_{80}.

The size of cubic P_4N_4 seems to match very well the inner cavity of the boron buckyball. Table 6 presents the bond distances and the bond angles of heteroatoms in the P_4N_4 complex. The bond distances are in the same range as the B−B bond distances in B_{80}, and the P−N bond calculated for hypothetical cubane-like P_4N_4 at the same level of theory B3LYP/SVP. The bond distances P−N and the bond angles in this complex are also close to the experimental data of diazaphosphetidine P_2N_2 reported by Chernega et al.[71] The cap boron atoms on the frame move inside the cage and form bonds with the P_4N_4 clusters. Concomitantly there is a large deviation of the displacement of the exohedral boron cap atoms of 0.15 Å. This illustrates the elastic coupling of endo and exo displacements in the I_h to T_h distortion mode.

b. $P_8@B_{80}$. P_8 keeps the cubane-like geometry (Figure 7) when encapsulated in B_{80}. The P−P bond distances are slightly contracted compared to the isolated P_8 and the P−B bond distance approaches the B−P bonds in the c-$P_4@B_{80}$ complex (see Table 7). The larger size of P_8 seems to be incompatible with

Table 6. Structural Parameters of the $P_4N_4@B_{80}$ Complex, B_{80}, P_4N_4, and P_2N_2[a]

	$P_4N_4@B_{80}$ (T)	B_{80}	P_4N_4 (T_d)	P_2N_2[71] expt
P−N bond lengths (Å)	1.84		1.81	1.59−1.66
P−N−P bond angles (deg)	94.15		92.07	95.40−95.65
N−P−N bond angles (deg)	85.69		87.90	84.27−84.68
B−B 6−5 bond lengths (Å)	1.67−1.80	1.76		
B−B 6−6 bond lengths (Å)	1.64−1.70	1.68		
nearest P−B bond distance (Å)	1.81			
center-nearest B	3.45 (0.22)	3.67		
center-furthest B	4.09 (0.15)	3.94		
central position of P_4N_4	yes			

[a] In parentheses are the deviations of nearest and furthest boron atoms to the references B_{80} caps.

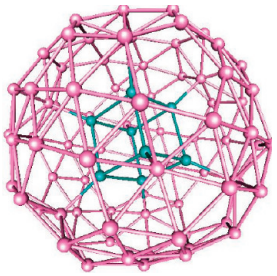

Figure 7. Optimized geometry of $P_8@B_{80}$ at B3LYP/6-31G(d).

Table 7. Structural Parameters of the $P_8@B_{80}$ Complex[a]

structural parameters	$P_8@B_{80}$ (T)	B_{80}	P_8 (O_h)
P−P bond lengths (Å)	2.11		2.13; 2.29[84]
P−B	1.76		
P−P−P bond angles (deg)	90		90; 90[84]
B−P−P bond angles (deg)	125.26		
B−B 6−5 bond lengths (Å)	1.72−1.77	1.76	
B−B 6−6 bond lengths (Å)	1.65−1.71	1.68	
center-nearest B	3.59 (0.08)	3.67	
center-furthest B	4.13 (0.19)	3.94	
central position of T_d P_8	yes		

[a] In parentheses are the deviations of nearest and furthest boron atoms to the reference B_{80} caps.

dx.doi.org/10.1021/jp107630q |J. Phys. Chem. A 2011, 115, 2268–2280

Table 8. Complexation Energies, NBO Charges Transferred between Guest Molecule and the Cage, and HOMO−LUMO Gap of Some Endohedral C_{84} Molecules at B3LYP/6-31G(d)

	C_{84}			B_{80}		
ligands	FE (kcal/mol)	charges transferred	HOMO−LUMO gap (eV)	FE (kcal/mol)	charges transferred	HOMO−LUMO gap (eV)
H_3N	−0.61	0.00	2.63	−27.09	0.39	1.82
H_3P	6.05	−0.01	2.63	−11.30	0.65	0.70
H_3As	−8.20	−0.01	2.64	5.83	0.12	1.97
H_4N_2	1.58		2.60	−24.35	0.37	1.75
H_3NBH_3	4.76	−0.03	2.60	−0.15	0.42	1.88
P_4	109.90	0.47	2.66	57.57	1.72	1.84
As_4	50.81	−0.02	2.60	124.73	1.67[a]	1.95
P_4N_4	155.66	−0.07	2.60	−32.87	2.23	1.96

[a] At B3LYP/STO-3G level.

the dimension of the B_{80} hollow cage. The deviations of boron cage are quite small. Fluck et al. found that the isolated P_8 is not stable and its destabilization energy compared to two P_4 molecules is almost 47 kcal/mol,[83] further Denk et al. studied the thermodynamic stability of P_8 using the CBS-Q method and revealed that the cuneane P_8 is more stable than the cubane form.[84] As P_8 is a nucleophile rich in electrons and the reactive caps on the B_{80} frame are electrophilic, the interaction between the two species is relatively strong to make this complex viable. However cubic P_8 is clearly too large and the complex is highly endothermic with an unfavorable complexation energy of 402 kcal/mol calculated at B3LYP/6-31G(d). The T_h-P_8@B_{80} shows two imaginary frequencies of e_u symmetry at the B3LYP/6-31G(d) level. We have distorted the geometry in the direction of these imaginary frequencies, which led to a lower C_i symmetry very close in energy with the T_h energy of −4713.8974 hartree. The frequencies analysis at the STO-3G level shows no imaginary vibrational modes.

c. P_4C_4@$B_{76}C_4$. In the P_4C_4@$B_{76}C_4$ complex, the encapsulated P_4C_4 keeps the same shape and each phosphorus atom is bound to one cap boron atom of the endo-76 cage, while the carbons are bound to the carbon caps (Figure S6, Supporting Information). The P_4C_4 cluster inside the cage has perfect cubic geometry characterized by a P−C bond length of 1.85 Å, and a PCP bond angle of 90°. The P−C and the C−C bond distances in the P_4C_4@B_{80} complex are short compared to the corresponding bonds and angles in $P_4C_4(CH_4)_3$ and $(terBut_3)_4P_4C_4$ computed at the same level of theory. This contraction of bonds of P_4C_4 inside the cage may destabilize the complex by increasing the strain energy in the cage. The calculated bond distances of tetra-*tert*-butyl phosphacubane are in the same range with the X-ray crystal structure.[85] However, Mo et al. analyzed the chemical reactivity of this compound and found that the carbon and the phosphorus are reactive sites for electrophilic reaction.[86] The B−B bonds in the complex are similar to the bond distances observed in endo-76. The cap endo and exohedral atoms move slightly inward and outward with respect to the reference position of the endo-76 molecule (Table S4, Supporting Information). The total electronic energy of this complex computed at the B3LYP/SVP level is about −3554.3050 hartree, the formation energy is around 23.84 kcal/mol. This amount is surprisingly small, taking into account the size of the encaged cluster.

d. B_4N_4@$B_{76}C_4$. The B_4N_4@$B_{76}C_4$ has a small HOMO−LUMO gap energy of 0.23 eV, which suggests the molecule to be highly reactive. The formation of this complex as is the case for several complexes studied in the present work is still endothermic. The B−N bonds of B_4N_4 in endo-76 are nearly 0.1 Å longer compared to the B−N bonds calculated in the free cubic B_4N_4 at different levels of theory.[87] The geometry of encaged B_4N_4 is slightly distorted with a BNB bond angle of 86.56°, a NBN angle of 93.34° and a B−N bond distance of 1.61 Å. The short B−N bond distance of nearly 1.50 Å between the donor B_4N_4 and the acceptor endo-76 is an illustration of the interaction between the cluster and the cage. However, the B_4N_4 molecule is quite small to seat comfortably in the middle of the cage.

F. Comparison with Encapsulation in Fullerenes: Endohedral NH_3, PH_3, AsH_3, H_4N_2, H_3BNH_3, P_4, and P_4N_4 Clusters Encaged in T_d-C_{84}. Several molecules and atoms have been experimentally enclosed in carbon fullerenes C_n. In order to compare the encapsulation properties of endohedral B_{80} with endohedral carbon fullerenes, a fullerene cage was required with similar size and symmetry characteristics as B_{80}. The tetrahedral leapfrog fullerene C_{84} fits very well with these criteria: it has a radius in between 3.96 and 4.43 Å, which lies in the same range with the size of B_{80} characterized by a mean radius of 4.14 Å, and it has symmetry T_d, versus T_h for B_{80}. An intensive encapsulation study of tetrahedral molecules of type MX_4 (ionic and neutral) and tetrahedral noble gas Ng_4 in C_{84} (T_d) has been performed by Charkin.[88] The ab initio calculations on endohedral C_{84} at the B3LYP/6-31G(d) level showed that the guest molecules P_4 and P_4N_4 both survived undeformed in C_{84} complexes, however with unfavorable formation energies of 109.90 and 155.66 kcal/mol, respectively and are minima on the potential energy surface with the smallest real frequencies corresponding to libration modes. Similar findings have been observed by Abdul[59] who reported that tetrahedral methane@C_{84} is 5.50 kcal/mol above the energy of the two separate molecules at the 6-31G(d)/BP86 level. Table 8 shows a trend comparing the formation energy of small molecules and tetrahedral molecules of group V encapsulated in C_{84} and in B_{80}. As it can be seen in this figure, C_{84} has different behavior compared to B_{80}. In contrast with the boron cage, C_{84} forms less stable complexes with hard bases compared to soft bases, and base molecules very rich in electrons are highly destabilized in C_{84}. On the other hand, weak bases are less affected by the nature of the hollow cages (B_{80} or C_{84}). The ammonia@C_{84} and hydrazine@C_{84} have neutral formation energy. The phosphine and ammonia borane molecules form metastables complexes with formation energy of 6.05 and 4.76 kcal/mol, respectively. Contrarily to B_{80}, arsine forms surprisingly a stable complex AsH_3@C_{84} characterized by a formation

dx.doi.org/10.1021/jp107630q |J. Phys. Chem. A 2011, 115, 2268–2280

Table 9. Mean Bond Distance between Heteroatom X and Nearest Boron Atom B (X−B) in Å, HOMO−LUMO Gap Energies in eV, Number of Imaginary Frequencies, Lowest Frequency in cm^{-1}, and Formation Energies (FE) in kcal/mol at the B3LYP/SVP Level and B3LYP/def-SVP Level for Sb−Boron Complexes[a]

compounds	sym (isomer)	X−B	gap	NI	low freq	FE
$N_4@B_{80}$	C_1 (a)	1.60	1.85	0	76	13.07
	C_1 (b)	3.12	1.96	0	52	5.13
$P_4@B_{80}$	T (a)	2.21	1.84	0	16	57.57
	C_1 (b)	2.05	0.69	0	145	45.52
	C_1 (c)	1.90	0.84	0	118	34.59
$P_2N_2@B_{80}$	C_1	1.86 (B−P)	0.88	0	120	−24.91
		1.52 (B−N)				
$P_3N@B_{80}$	C_1 (a)	1.44 (B−N)	0.87	0	162	3.77
		2.01 (B−P)				
	C_1 (b)	1.98 (B−P)	0.83	0	96	1.13
		1.60 (B−N)				
$As_4@B_{80}$	T (a)	2.40	1.95	3	*i73*	124.73
	C_2 (b)	2.01	0.67	2	*i193*	111.52
	C_1 (c)	2.07	0.79	0	103	107.29
	C_1 (d)	2.06	0.86	0	121	111.24
$Sb_4@B_{80}$	T (a)	2.27	0.40	20	*i1877*	463.60
	T (c)	2.58	0.61	12	*i2196*	477.41
	C_1 (bis)	2.21	1.06	0	90	268.20
adamant@endo76	T	1.53 (C−C)[b]	1.93	0	97	515.81
B_{80}[2]	T_h		1.96	0		

[a] The frequency single point calculation of lower symmetry has been performed at lower level B3LYP/STO-3G. [b] Bond distance between carbon of adamentane and cap carbon atom of endo-76.

energy of −8.20 kcal/mol. C_{84} acts like a soft electron acceptor and prefers soft base not very rich in electrons. Carbon atoms are a little neutral and tend to repel electrons from guest rich electron system as P_4N_4. The repulsion interaction between the encapsulated molecules and the wall frame appears to be strong when the electron density of the guest molecule increases. The strain energy is small since the encapsulated molecules stay at the middle of the cage and the geometrical parameters of these complexes are similar to the geometry of their isolated components. All encapsulated molecules do not transfer any electrons to the cage except P_4, which gives nearly half an electron to the C_{84} frame. This suggests a weak interaction between guest molecules and the cage. Two factors seem to play a crucial role in stabilization effects, first the polarizability of the molecule and second the basicity. The difference between the C_{84} and B_{80} cages illustrated by the difference in formation energies is small with encapsulated weak base as ammonia borane.

DISCUSSION

The present results confirm the original hypothesis that—contrary to buckminsterfullerene—B_{80} offers new possibilities for endohedral bond formation, due to the presence of suitably oriented capping atoms. However only very few complexes have been verified to give rise to negative complexation energy. Size seems to be a critical parameter, which destabilizes the complex by exerting an internal strain that couples to the highly energetic breathing mode of the boron cage. A comparison of the decomposition energies with emphasis on size effects is presented

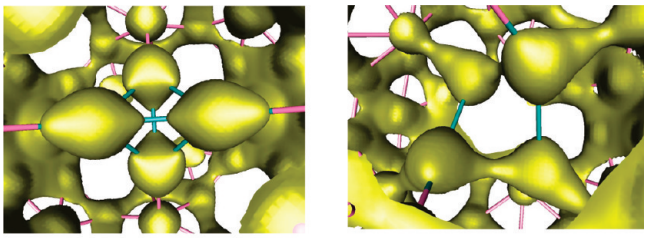

Figure 8. Section of total electron densities of $P_4@B_{80}$ complexes: (a) tetrahedral P_4; (b) bisphenoidal P_4.

below. Even if the internal energy of large encapsulated clusters may be very high, the resulting compounds have a high metastability, since the strong boron−boron bonds on the surface of the cluster will prevent decomposition.

a. Tetrahedral $X_4@B_{80}$ Complexes (X = N, P, As, Sb, Adamantane). In Table 9, the total energies, the gap between the energies of the HOMO and the LUMO, the presence of imaginary frequencies and the values of the formation energies of various tetrahedral complexes studied in this paper are presented. All complexes composed of tetrahedral cluster of family V embedded in B_{80} have positive complexation energies and their formation is endothermic, except the $P_2N_2@B_{80}$. As can be seen in this table, the complexation energies increase with the size and the orientation inside the cage of the encapsulated tetrahedral clusters. The maximum positive value of the tetrahedral group V family is observed for antimony. As in the case of its homologues $N_4@C_{60}$ and $N_4@C_{80}$, the formation of $N_4@B_{80}$ is endothermic with an inclusion energy in the range of 5−13 kcal/mol. The low frequency mode in the off centered-$N_4@B_{80}$ complex (C_1a) involves the N_4 and looks quite similar to the simple pendulum motion. The lowest frequency of tetrahedral $P_4@B_{80}$ is associated with a twisting mode and like in the $N_4@B_{80}$ complex only the heteroatoms contribute to the vibration motion. The centered $N_4@B_{80}$ complex (C_1b) corresponds to an encapsulated minimum with very low complexation energy of 5.13 kcal/mol. The $As_4@B_{80}$ and $Sb_4@B_{80}$ complexes are thermodynamically unstable with decomposition energies respectively of 107.29 and 268.20 kcal/mol. Clearly, the antimony cluster has become too large to form even a metastable encapsulation.

The total electron density map shows electron density built-up in the region of the B−P and P−P bonds in $P_4@B_{80}$ (Figure 8a, b) for tetrahedral and bisphenoidal symmetry. In the bisphenoid (Figure 8b) complex two types of B−P bonds are expected with a different degree of covalency. The phosphorus in this complex tends to form strong bonds with cap boron atoms. This leads to an elongation of the P−P bond distance, which decreases the interaction between P−P atoms. Unlike in the bisphenoidal P_4 complex, the tetrahedral structure shows a depletion of electrons in the P−B region. Referring to the number of electrons where on average 0.5 electrons were transferred per phosphorus in the tetrahedral complex, we can suggest a weak tendency of ionic interaction between the phosphorus atoms and the deficient cap boron atoms. This may be illustrated by the lack of electrons in the B−P region. With a difference in P−P bonds of 0.05 Å compared to the bisphenoid complex, the P−P bonds in the tetrahedral complex do not interact strongly. The HOMO of $P_4@B_{80}$ in tetrahedral symmetry is similar to the HOMO of B_{80}, with virtually no contributions of the P_4 cluster (Figure 9a). In contrast in the LUMO, the frontier orbitals of P_4 are dominant

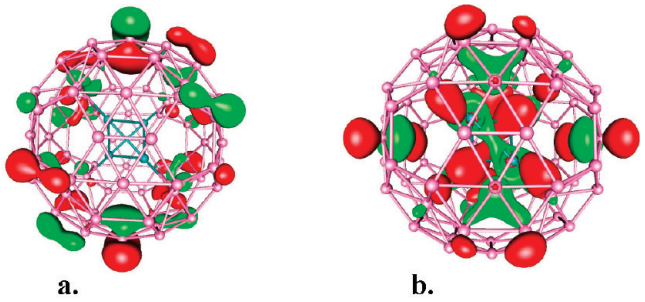

Figure 9. $P_4@B_{80}$ frontier molecular orbitals: (a) HOMO; (b) LUMO.

Table 10. Mean Bond Distances between Heteroatom and Nearest Cap Boron Atom (X−B) in Å, HOMO−LUMO Gap Energies in eV, Number of Imaginary Frequencies, and Lowest Frequency in cm^{-1}, and Formation Energies (FE) in kcal/mol at B3LYP/SVP

compounds	sym	X−B	gap	NI	low freq	F.E
P_4C_4@endo76	T	1.47 (C−C)	2.57	0	163	23.84
		1.81 (B−P)				
$P_4N_4@B_{80}$	T	1.57 (B−N)	1.96	0	174	−32.87
		1.805 (B−P)				
B_4N_4@endo76	T	1.50 (B−N)	0.23	0	133	187.17
		1.615 (B−C)				
$P_8@B_{80}$	C_1	1.77	2.04	0	72[a]	401.83
B_{80}^{2}	T_h		1.96	0		

[a] Frequency single point calculation at the B3LYP/STO-3G level.

(Figure 9b). The N_4 cluster does not contribute to the frontier molecular orbitals of the $N_4@B_{80}$ complex (Figure S7a,b, Supporting Information). Similar results have been observed in $N_4@C_{60}$ and $N_4@C_{80}$ complexes. Tetrahedral clusters of the V family transfer electrons to the B_{80} cage. The lowest amount is observed with N_4. The total number of electrons shared between the P_4 cluster and the B_{80} computed with the NBO program averages 2 electrons.

b. Endohedral Cubane-Like Analogues. The total energies, the HOMO−LUMO gap energies, the number of imaginary frequencies and the formation energies of different cubic donor−acceptors complexes are illustrated in Table 10. Except for the $P_4N_4@B_{80}$ complex, all complexes in the table are unfavorable thermodynamically. The $P_8@B_{80}$ complex optimized at B3LYP/SVP with no symmetry constraints has all vibrational modes real at the lower level, but the high formation energy suggests that the P_8 cluster is too big to be in the cage and its formation requires huge energy. The P_4C_4 in the endo-76 cage requires only 23.84 kcal/mol. This quantity is small compared to the size of the molecule and the value of the total electronic energy of the complex. We have plotted the frontier orbitals of the $P_4N_4@B_{80}$ complex in (Figure 10). The HOMO is quite similar to the HOMO of the boron buckyball B_{80}, the contribution of P_4N_4 to the HOMO is weak, unlike the LUMO which shows an important contribution of phosphorus and nitrogen atoms. The frontier orbitals of $P_4C_4@B_{76}C_4$ show that P_4C_4 contributes slightly to the construction of the HOMO, in contrast with $P_4N_4@B_{80}$ the LUMO of $P_4C_4@B_{80}$ is essentially localized on the B_{80} cage (Figure S8a,b, Supporting Information). Figure 11 presents the total electron densities of the most stable complex. The six boron four-center bond motifs observed in other stables

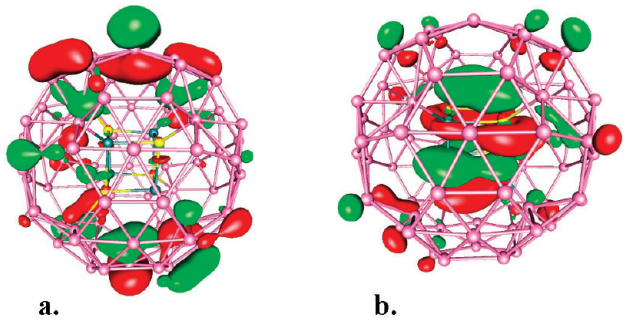

Figure 10. Frontier molecular orbitals of the $P_4N_4@B_{80}$ complex: (a) HOMO; (b) LUMO.

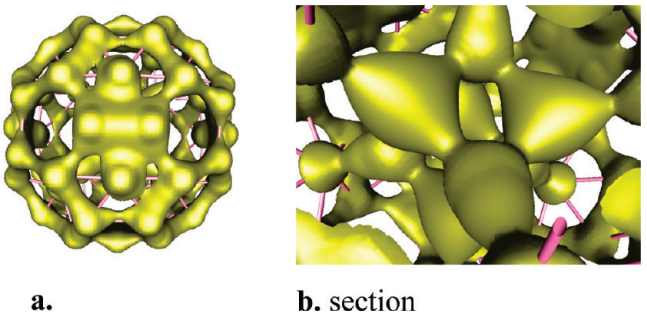

Figure 11. (a) Total electronic densities of the $P_4N_4@B_{80}$ complex. (b) Section of part a.

structures[9] such as B_{80}, endo-76 and endo-72 are also present in the $P_4N_4@B_{80}$ complex. The P_4N_4 transferred 2.23 electrons to the cage. In this cluster the Phosphorus atoms are equally charged with a positive charge per atom of 1.96; in contrast with the nitrogen atoms, which have a negative charge of −1.40. The phosphorus centers are highly reactive for electrophilic attack. The stability of the $P_4N_4@B_{80}$ complex is due to its size and its ability to share electrons with the electron deficient cap boron atoms. The P_8 transfers the highest number of electrons to B_{80} through the 8 B−P bonds and tends to stabilize the complex. But the strain energy of this complex is very strong given the dimension of the hollow B_{80} and the large size of P_8.

The comparison between B_{80} and the C_{84} fullerene with similar size clearly shows the large difference in bonding characteristics of the endohedral cage. The fullerene bonding is limited to weak interactions, mainly dictated by polarizability. In contrast in the boron buckyball effective chemical bonds are established between group V heteroatoms and acidic boron sites. The tetrahedral P_4, and P_4N_4 complexes are strongly destabilizing in C_{84}. The majority of base molecules of Group V are metastable in C_{84} except AsH_3, which shows higher polarizability.

■ CONCLUSION

In this paper, we have presented a computational study of the encapsulation of tetrahedral and cubane-like clusters in the boron buckyball. All clusters included group V elements, which may form donor−acceptor bonds with the endohedral boron caps. Among the cubane-like complexes, $P_4N_4@B_{80}$ is thermodynamically the most stable with a large HOMO−LUMO gap. In the tetrahedral series, most complexes are unfavorable except $P_2N_2@B_{80}$; although encapsulation of N_4 and of mixed PN_3 clusters are almost thermoneutral. Probably N_4 is too small to be

stabilized in the middle of the cage, while on the other hand P_4 appears as a soft base. B_{80} itself is considered as a hard acid. The As_4 and Sb_4 tetrahedra are definitely too large as compared to the free volume in the cage and exert, like the adamantane complex, serious strains on the cage. The volume of the B_{80} hollow is rather sufficient to stock small molecules and to realize some reactions inside. The NH_3, PH_3, N_2H_4, and $BH_3{-}NH_3$ can form viable stable complexes with the boron buckyball. The investigation of the chemical reaction of some small molecules inside the cage will be very interesting for further researches to elucidate the reactivity of B_{80}. From a catalytic point of view the cavity inside B_{80} proves to be a very special microenvironment, which can activate unusual bonding modes. Most interesting in this respect is perhaps the PH bond dissociation in PH_3 upon addition to the inner wall.

■ ASSOCIATED CONTENT

Supporting Information. Additional computational details including geometrical parameters, frontier molecular orbitals, shapes of tetrahedral and cubane-like optimized geometries. This material is available free of charge via the Internet at http://pubs.acs.org.

■ AUTHOR INFORMATION

Corresponding Author

*E-mail: Jules.Tshishimbi@chem.kuleuven.be.

■ ACKNOWLEDGMENT

The authors thank the KULeuven Research council and the Flemish Science Fund (FWO-Vlaanderen) for financial support.

■ REFERENCES

(1) Szwacki, N. G.; Sadrzadeh, A.; Yakobson, B. I. *Phys. Rev. Lett.* **2007**, *98*, 166804.
(2) Gopakumar, G.; Nguyen, M. T.; Ceulemans, A. *Chem. Phys. Lett.* **2008**, *450*, 175.
(3) Prasad, D. L. V. K.; Jemmis, E. D. *Phys. Rev. Lett.* **2008**, *100*, 165504.
(4) Baruah, T.; Pederson, M. R.; Zope, R. R. *Phys. Rev. B* **2008**, *78*, 045408.
(5) Ceulemans, A.; Muya, J. T.; Gopakumar, G.; Nguyen, M. T. *Chem. Phys. Lett.* **2008**, *426*, 226.
(6) Yan, Q.; Zheng, Q.; Su, G. *Phys. Rev. B* **2008**, *77*, 224106.
(7) Li, Y.; Zhou, G.; Li, J.; Gu, B.; Duan, W. *J. Phys. Chem. C* **2008**, *112*, 19268.
(8) Zope, R. R.; Baruah, T. *Phys. Rev .B* **2009**, *80*, 033410.
(9) Muya, J. T.; Nguyen, M. T.; Ceulemans, A. *Chem. Phys. Lett.* **2009**, *483*, 101.
(10) Botti, S.; Castro, A.; Lathiotakis, N. L.; Andrade, X.; Marques, M. A. L. *Phys. Chem. Chem. Phys.* **2009**, *11*, 4523.
(11) Liu, A. Y.; Zope, R. R.; Pederson, M. R. *Phys. Rev. B* **2008**, *78*, 155422.
(12) Boustani, I.; Karna, S. P. *J. Phys. Chem. C* **2010**, *114*, 4149.
(13) Li, M.; Li, Y.; Zhou, Z.; Shen, P.; Chen, Z. *Nano Lett.* **2009**, *9*, 1944.
(14) Wu, G.; Wang, J.; Zhang, X.; Zhu, L. *J. Phys. Chem. C* **2009**, *113*, 7052.
(15) Zhao, Y.; Lusk, M. T.; Dillon, A. C.; Heben, M. J.; Zhang, S. B. *Nano Lett.* **2008**, *8*, 157.
(16) Ross, R. B.; Cardona, C. M.; Guldi, D. M.; Sankaranarayanan, S. G.; Reese, M. O.; Kopidakis, N.; Peet, J.; Walker, B.; Bazan, G. C.; Keuren, E. V.; Holloway, B. C.; Drees, M. *Nat. Mater.* **2009**, *8*, 208.
(17) Li, H.; Shao, N.; Shang, B.; Yuan, L.-F.; Yang, J.; Zeng, X. C. *Chem. Commun.* **2010**, *46*, 3878.
(18) Zhao, J.; Wang, L.; Li, F.; Chen, Z. *J. Phys. Chem. A* **2010**, *114*, 9969.
(19) Cardona, C. M.; Elliott, B.; Echegoyen, L. J. *J. Am. Chem. Soc.* **2006**, *128*, 6480.
(20) Stevenson, S.; Rice, G.; Glass, T.; Harich, K.; Cromer, F.; Jordan, M. R.; Craft, J.; Hadju, E.; Bible, R.; Olmstead, M. M.; Maitra, K.; Fisher, A. J.; Balch, A. L.; Dorn, H. C. *Nature* **1999**, *401*, 55.
(21) MacFarland, D. K.; MacFarland, D. K.; Walker, K. L.; Lenk, R. P.; Wilson, S. R.; Kumar, K.; Kepley, C. L.; Garbow, J. R. *J. Med. Chem.* **2008**, *51*, 3681.
(22) Jones, M. A. G.; Taylor, R. A.; Ardavan, A.; Porfyrakis, K.; Briggs, G. A. D. *Chem. Phys. Lett.* **2006**, *428*, 303.
(23) Campanera, J. M. C.; Olmstead, M. M.; Balch, A. L.; Poblet, J. M. *J. Phys. Chem. A* **2002**, *106*, 12356.
(24) Ge, Z.; James, C. D.; Cai, T.; Gibson, H. W.; Harry, C. D. *J. Am. Chem. Soc.* **2005**, *127*, 16292.
(25) Xiao-Yuan, R.; Zi-Yang, L. *Struct. Chem.* **2005**, *16*, 567.
(26) Li, B.; Xu, Z. *J. Am. Chem. Soc.* **2009**, *131*, 16380.
(27) Peng, S.; Li, X. J.; Zhang, D. X.; Zhang, Y. *Struct. Chem.* **2009**, *20*, 789.
(28) Wang, T.; Chen, N.; Xiang, J.; Li, B.; Wu, J.; Xu, W.; Jiang, L.; Tan, K.; Shu, C.; Lu, X.; Wang, C. *J. Am. Chem. Soc.* **2009**, *131*, 16646.
(29) Li, J. L.; Yang, G. W. *J. Phys. Chem. C* **2009**, *113*, 18292.
(30) Li, J. L.; Yang, G. W. *Appl. Phys. Lett.* **2009**, *95*, 133115.
(31) Jin, P.; Hao, C.; Gao, Z.; Zhang, S. B.; Chen, Z. *Phys. Chem. A* **2009**, *113*, 11613.
(32) Prasad, D. L. V. K.; Jemmis, E. D. *Appl. Phys. Lett.* **2010**, *96*, 023108.
(33) Schäfer, A.; Horn, H.; Ahlrichs, R. *J. Chem. Phys.* **1992**, *97*, 2571.
(34) Weigend, F.; Ahlrichs, R. *Phys. Chem. Chem. Phys.* **2005**, *7*, 3297.
(35) Weigend, F. *Phys. Chem. Chem. Phys.* **2006**, *8*, 1057.
(36) Frisch, M. J.; et al. , *Gaussian 03, Rev.D02*, Gaussian, Inc.: Wallingford CT, 2004.
(37) Ahlrichs, R.; Bär, M.; Häser, M.; Horn, H.; Kölmel, C. *Chem. Phys. Lett.* **1989**, *162*, 165.
(38) Laaksonen, L. *J. Mol. Graph.* **1992**, *10*, 33.
(39) Bergman, D. L.; Laaksonen, L.; Laaksonen, A. *J. Mol. Graph.* **1997**, *15*, 301.
(40) http://www.cmbi.ru.nl/molden/
(41) Foster, J. P.; Weinhold, F. *J. Am. Chem. Soc.* **1980**, *102*, 7211.
(42) Biegler-König, F.; Schönbohm, J.; Bayles, D. *J. Comput. Chem.* **2001**, *22*, 545.
(43) Murphy, T. A.; Pawlik, T.; Weidinger, A.; Hihne, M.; Alcala, R.; Spaeth, J. M. *Phys. Rev. Lett.* **1996**, *77*, 1075.
(44) Knapp, C.; Weiden, N.; Ka, H.; Dinse, K.-P.; Pietzak, B.; Waiblinger, M.; Weidinger, A. *Mol. Phys.* **1998**, *95*, 999.
(45) Weidinger, A.; Waiblinger, M.; Pietzak, B.; Almeida Murphy, T. *Appl. Phys. A: Mater. Sci. Process* **1998**, *A66*, 287.
(46) Dietel, E.; Hirsch, A.; Pietzak, B.; Waiblinger, M.; Lips, K.; Weidinger, A.; Gruss, A.; Dinse, K. P. *J. Am .Chem. Soc.* **1999**, *121*, 2432.
(47) Nguyen, V. S.; Matus, M. H.; Nguyen, M. T.; Dixon, D. A. *J. Phys. Chem. A* **2008**, *112*, 9946.
(48) Durig, J. R.; Li, Y. S.; Carreira, L. A.; Odom, J. D. *J. Am. Chem. Soc.* **1973**, *95*, 2491.
(49) Anane, H.; Jarid, A.; Boutalib, A.; Nebot-Gil, I.; Tomas, F. *Chem. Phys. Lett.* **1998**, *296*, 277.
(50) Pearson, R. G. *Science* **1966**, *151*, 172.
(51) Schlegel, H. B.; Skancke, A. *J. Am. Chem. Soc.* **1993**, *115*, 7465.
(52) Lee, T. J.; Rice, J. E. *J. Chem. Phys.* **1991**, *94*, 1215.
(53) Yarkony, D. R. *J. Am. Chem. Soc.* **1992**, *114*, 5406.
(54) Ren, X.; Liu, Z. *Struct. Chem.* **2005**, *16*, 6.
(55) Chun-Mei, T.; Wei-Hua, Z.; Kai-ming, D. *Chin. Phys. Lett.* **2009**, *26*, 096101.
(56) Bitterova, M.; Brink, T.; Ostmark, H. *J. Phys. Chem. A* **2000**, *104*, 11999.

(57) Leininger, M. L.; Huis, T. J. V.; Schaefer, H. F. *J. Phys. Chem. A* **1997**, *101*, 4460.
(58) Li, L.; Shang, J.; liu, J.; Wang, X.; Wong, N. *J. Mol. Struct. (THEOCHEM)* **2007**, *807*, 207.
(59) Rehaman, A.; Gagiliardi, L.; Pyykko, P. *Int. J. Quantum Chem.* **2007**, *107*, 1162.
(60) Charkin, O.; Klimenko, N.; Charkin, D.; Mebel, A. *Zh. Neorg. Khim.* **2004**, *49*, 792.
(61) Kuganathan, N. *Int. J. Nanotech.* **2009**, *3*, 1.
(62) Kobayashi, K.; Nagase, S.; Dinse, K. *Chem. Phys. Lett.* **2003**, *377*, 93.
(63) Mal, P.; Breiner, B.; Rissanen, K.; Nitschke, J. R. *Science* **2009**, *324*, 1697.
(64) Tsirelson, V. G.; Tarasova, N. P.; Bobrov, M. F.; Smetannikov, Yu.V. *Heteroat. Chem.* **2006**, *17*, 572.
(65) Bader, R.F.W., *Atoms in Molecules: A quantum Theory*; Clarendon Press: Oxford, U.K., 1994.
(66) Bader, R. F. W.; Lee, T. S.; Cremer, D.; Kraka, E. *J. Am. Chem. Soc.* **1983**, *105*, 5061.
(67) Bader, R. F. W.; Tang, T.; Tal, Y.; Biegler-König, F. W. *J. Am. Chem. Soc.* **1982**, *104*, 946.
(68) Grimme, S. *J. Am. Chem. Soc.* **1996**, *118*, 1529.
(69) Marabello, D.; Bianchi, R.; Gervasio, G.; Cargnoni, F. *Acta Crystallogr.* **2004**, *60*, 494.
(70) Kwon, O.; Almond, P. M.; McKee, M. L. *J. Phys. Chem. A* **2002**, *106*, 6864.
(71) Chernega, A. N.; Antipin, M. Yu.; Struchkov, Yu. T.; Bodelskul, I. E.; Marchenko, A. P.; Pinchuk, A. M. *Zh. Struk. Khim.* **1985**, *28*, 135.
(72) Hohm, U.; Goebel, D.; Karamanis, P.; Maroulis, G. *J. Phys. Chem. A* **1998**, *102*, 8.
(73) Wiberg, E., Wiberg, N., Holleman, A. F. *Inorg. Chem.*: Academic Press: San Diego, CA, 2001.
(74) Toyoda, K.; Hiraoka, Y. S.; Naritsuka, S.; Nishinaga, T. *Appl. Surf. Sci.* **2000**, *159*, 360.
(75) Morino, Y.; Ukaji, T.; Ito, T. *Bull. Chem. Soc. Jpn.* **1966**, *39*, 64.
(76) Zhao, J.; Zhou, X.; Chen, X. *Phys. Rev. B* **2006**, *73*, 115418.
(77) Chadha, R. K.; Chehayber, J. M.; Drake, J. E. *J. Chem. Cristallogr.* **1985**, *15*, 53.
(78) Zhang, H.; Balasubramanian, K. *J. Chem. Phys.* **1992**, *97*, 3437.
(79) Zhou, X.; Zhao, J.; Chen, X.; Lu, W. *Phys. Rev. A* **2005**, *72*, 053203.
(80) Marsusi, F.; Mirabbaszadeh, K.; Mansoori, G. A. *Physica E* **2009**, *41*, 1151.
(81) Breza, M. *J. Mol. Struct. (THEOCHEM)* **2004**, *679*, 131.
(82) Elias, A. J.; Twamley, B.; Haist, R.; Oberhammer, H.; Henkel, G.; Krebs, B.; Lork, E.; Mews, R.; Shreeve, J. M. *J. Am. Chem. Soc.* **2001**, *123*, 10299.
(83) Fluck, E.; Pavlidou, C. M. E.; Janoschek, R. *Phosphorus Sulphur* **1979**, *6*, 469.
(84) Denk, M. K.; Hezarkhani, A. *Heteroatom. Chem.* **2005**, *16*, 458.
(85) Greenberg, A., Liebman, J. F. *Strained organic molecules*: Academic Press: New York, 1978.
(86) Mo, O.; Yáñez, M. *Can. J. Chem.* **1996**, *74*, 901.
(87) Manaa, M. R. *J. Mol. Struc, (THEOCHEM)* **2001**, *549*, 23.
(88) Charkin, O. P.; Klimenko, N. M.; Charkin, D. O.; Mebel, A. M.; Lin, S. H. *Russ. J. Inorg. Chem.* **2006**, *51*, 1.